

Articles

Kinetic and Mechanistic Studies of L-Lactide Polymerization in Supercritical Chlorodifluoromethane

Ji Won Park,^{†,‡} Soo Hyun Kim,^{*,†} Soo Young Park,[‡] Youn-Woo Lee,[§] and Young Ha Kim[†]

Biomaterials Research Center, Korea Institute of Science and Technology, P.O. Box 131, Cheongryang, Seoul 130-650, South Korea; School of Materials Science and Engineering, Seoul National University, San 56-1, Shilim-dong, Kwanak-gu, Seoul, 151-742, Korea; and Supercritical Fluid Research Laboratory, Korea Institute of Science and Technology, P.O. Box 131, Cheongryang, Seoul 130-650, South Korea

Received July 1, 2003; Revised Manuscript Received September 19, 2003

ABSTRACT: The ring-opening polymerization of L-lactide (L-LA) initiated by 1-dodecanol/tin(II) octoate was carried out in supercritical chlorodifluoromethane at 110 °C under a pressure of 200 bar. MALDI-TOF mass spectroscopy and ¹H NMR studies suggested that polymerization proceeded via a traditional coordination–insertion mechanism involving a tin alkoxide bond and the cleavage of the acyl–oxygen bond of the monomer. The polymerization was controlled using the linear relation between $\ln([LA]_0/[LA])$ on the polymerization time and the molecular weight on conversion. The relative polymerization rate constants increased with increasing tin(II) octoate and 1-dodecanol concentrations. Gel permeation chromatography analysis indicated that the molecular weight distribution was bimodal, at least for certain monomer conversion. The bimodal distribution may be a result of specific intermolecular interactions between chlorodifluoromethane and hydroxyl groups on 1-dodecanol or on dormant macromolecules. The mechanisms of the initiation and chain transfer steps of L-lactide polymerization in supercritical chlorodifluoromethane are proposed.

Introduction

The use of supercritical carbon dioxide (scCO₂) as a solvent for polymerization is attractive because of its low toxicity, cost, and nonflammability.¹ Several common polymers have been synthesized in scCO₂; these include fluoropolymers, polysiloxanes, poly(methyl methacrylate), polystyrene, and polycarbonates, as reviewed elsewhere.^{2,3} These polymerizations are either homogeneous or heterogeneous in nature, depending on the solubility of the polymer in scCO₂.⁴ Unfortunately, many polymers other than specific fluoropolymers and polysiloxanes have limited solubility in scCO₂, which reduces possible homogeneous polymerizations to an extremely narrow range.⁵ Thus far, most studies have focused on heterogeneous-phase polymerizations and on the development of new surfactants.⁶ Recently, cloud point measurements by Lee et al.^{7,8} suggested that poly(L-lactide) (PLLA) is readily soluble in chlorodifluoromethane (R22) due to the specific interaction between the hydrogen atoms of R22 and the polymer ester group.^{9,10} Thus, the ring-opening polymerization (ROP) of L-lactide (L-LA) in supercritical chlorodifluoromethane (scR22) allows high degrees of monomer conversion and

high MWs in a homogeneous phase.¹¹ An attractive feature of R22 is its lower ozone depletion than chlorofluorocarbons;¹² in fact, it is used in medical applications. Recently, Cooper et al.¹³ reported that cross-linked PMMA is produced by dispersion polymerization in 1,1,1,2-tetrafluoroethane, the more acceptable hydrofluorocarbons.

It has been demonstrated that lactone polymerization using aluminum and tin alkoxides proceeds via a coordination–insertion mechanism.¹⁴ When tin(II) octoate (Sn(Oct)₂) is used as a catalyst, without alkoxide (or hydroxide) groups in a pure state, it has been proposed that Sn(Oct)₂ react with alcohol and are converted to tin alkoxides, which are active species in the polymerization.^{15–18} Therefore, a coordination–insertion mechanism was postulated for the catalytic activity of Sn(Oct)₂, which involves a covalent tin alkoxide bond and the cleavage of the acyl–oxygen bond of the lactone. It was also reported that the rate-determining step in the coordination–insertion mechanism is the nucleophilic attack of the tin alkoxide on the carbonyl carbon of the monomer.¹⁹ Furthermore, when the ROP of lactone was carried out in polar solvent, the kinetics of the lactone polymerization showed longer induction times or lower polymerization rates.^{14,20} This has been attributed to competition between the monomer and solvent for coordination to the alkoxide. The structures of active species, the equilibria between them, and their contribution to propagation and intra-/intermolecular transesterification are known for the coordination–insertion mecha-

[†] Biomaterials Research Center, Korea Institute of Science and Technology.

[‡] Seoul National University.

[§] Supercritical Fluid Research Laboratory, Korea Institute of Science and Technology.

* Corresponding author: Tel +82-2-958-5343; Fax +82-2-958-5308; e-mail soohkim@kist.re.kr.

nism of lactone with tin-based initiation systems in solution, in bulk, and in heterogeneous scCO_2 systems.^{21–23} However, nothing is known about the mechanism and the kinetics of the homogeneous ROP of L-LA in scR22 .

In this paper, we report preliminary results about the ROP of L-LA initiated by 1-dodecanol/ $\text{Sn}(\text{Oct})_2$ in scR22 . This research illustrates the structures of active species, the equilibria between them, and their contribution to the propagation reaction in scR22 .

Experimental Section

Materials. L-Lactide (L-LA) was purchased from Purac Biochem BV (Gorinchem, The Netherlands) and was recrystallized from ethyl acetate and dried in a vacuum (0.2 mmHg) over P_4O_{10} . Tin(II) bis(2-ethylhexanoate) ($\text{Sn}(\text{Oct})_2$) (Sigma Chemical Co., St. Louis, MO, 99%) and 1-dodecanol (DoOH) (Aldrich, 99.5%) were purified by distillation under reduced pressure and dissolved in dry toluene. R22 was purchased from the Solvay Gas Co. and had a certified purity of 99.99 wt %; it was used as received without further purification. Toluene was dried by refluxing over the benzophenone–Na complex and distilled under a nitrogen atmosphere just prior to use. CDCl_3 (Aldrich, 99.5 atom % D) was used as received.

Polymerization Procedure in Supercritical R22 (scR22). Polymerization was conducted in a 52 mL stainless steel high-pressure cell equipped with a magnetic stirring bar and an electrically heating mantle. L-LA (3.0 g), DoOH solution (0.3 mL of a 0.11 M solution in toluene; 3.3×10^{-5} mol of DoOH), and $\text{Sn}(\text{Oct})_2$ solution (0.43 mL of a 0.12 M solution in toluene; 5.2×10^{-5} mol of $\text{Sn}(\text{Oct})_2$) were added to the cell. The toluene was removed under vacuum, and the reactor was then heated to 50 °C and purged with nitrogen for 5 min. When the reactor was cooled to room temperature, it was evacuated for 2 h using a liquid nitrogen cooled trap and then purged with nitrogen for an additional 10 min. The cell was then disconnected from the nitrogen line, evacuated, and connected to the R22 feed system. The cell was filled with liquid R22 to ca. 30 bar at 50 °C by using an air-driven gas compressor (Maximator Schmidt Kranz & Co. GmbH) and then gradually heated to 110 °C to achieve a pressure of 200 bar. Polymerization was allowed to proceed for the predetermined times. After the polymerization, the reactor was cooled to room temperature, and R22 was vented through a needle valve into chloroform in order to collect both unreacted monomer and polymer. To quantify L-LA conversion, the cell was rinsed with chloroform in order to dissolve traces of the polymer and monomer. Both chloroform solutions were poured into a large volume of cold methanol; the precipitated PLLA was recovered by filtration and dried under vacuum at room temperature to constant weight. Monomer conversion was determined gravimetrically.

Polymerization of L-LA in Bulk. Bulk polymerizations were carried out in flame-dried 50 mL glass ampules. L-LA was weighed into the glass ampules, which were equipped with a magnetic stirring bar. L-LA (3.0 g), DoOH solution (0.3 mL of a 0.11 M solution in toluene; 3.3×10^{-5} mol of DoOH), and $\text{Sn}(\text{Oct})_2$ solution (0.43 mL of a 0.12 M solution in toluene; 5.2×10^{-5} mol of $\text{Sn}(\text{Oct})_2$) were added to the ampules, which were then heated under reduced pressure with a heat gun to remove toluene and purged with dry N_2 gas three times. The ampules were then sealed and heated in a silicone oil bath. After the reaction the ampules were broken, and the polymers were dissolved in chloroform and precipitated in methanol. The precipitated polymers were filtered off and dried under vacuum at room temperature to constant weight.

Determination of Molar Masses (M_n) and of Polydispersity Indexes (M_w/M_n). Molecular weight (MW) and molecular weight distribution (MWD) were determined by gel permeation chromatography (GPC) using a Waters150-C equipped with a Waters 510 fluid unit and a Waters 410 differential refractometer. A combination of three Shodex microstyragel columns with molecular weight exclusion limits

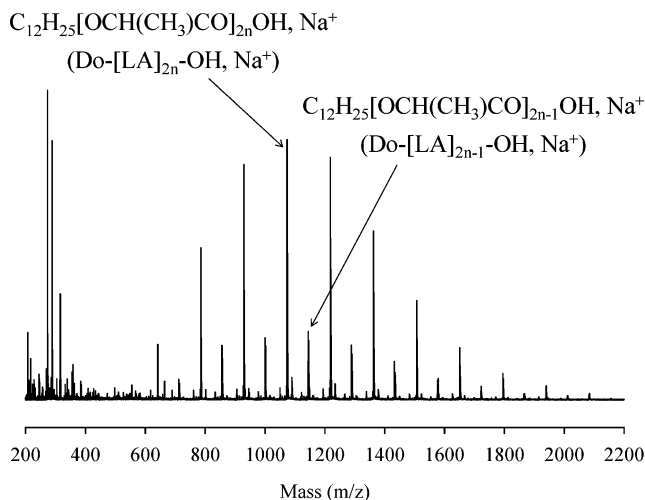


Figure 1. MALDI-TOF spectrum of the low molecular weight poly(L-lactide). Polymerization condition: $[\text{LA}]_0 = 0.4$ mol/L, $[\text{LA}]_0/[\text{DoOH}]_0 = 9.7$, and $[\text{DoOH}]_0/[\text{Sn}]_0 = 0.2$; at 110 °C, 200 bar in supercritical chlorodifluoromethane.

of 1500/70 000/400 000 g/mol was used. The column were eluted with CHCl_3 (flow rate 1.0 mL/min at 30 °C) and calibrated with polystyrene standards over a MW range of 1000–350 000.

NMR Measurements. ^1H NMR spectra were recorded at 25 °C using a Varian Unity Plus 300 MHz spectrometer in CDCl_3 . TMS was used as an internal reference.

MALDI-TOF Measurements. Mass spectrometric measurements were performed using a Voyager Elite (PerSeptive Biosystems, Farmingham, MA) time-of-flight instrument equipped with a pulsed N_2 laser (337 nm, 4 ns pulse width), a time-delayed extraction ion source, and an accelerating voltage of 20 kV. Mass spectra were recorded in the reflector mode. The matrix, 2,5-dihydroxybenzoic acid, was dissolved in THF (10 mg/mL), and the solution was mixed with the polymerization mixture (monomer concentration in the feed: 1.0 mol/L) in a 20:1 v/v ratio. The mixture was dried on a stainless steel plate, which was covered by the gold target.

Results and Discussion

Mechanism of L-LA Polymerization Initiated by DoOH/ $\text{Sn}(\text{Oct})_2$ in scR22 . Recently, it was reported that the ring-opening polymerization (ROP) of cyclic ester initiated tin(II) octoate ($\text{Sn}(\text{Oct})_2$) involves a coordination–insertion mechanism with selective cleavage of the acyl–oxygen bond of the monomer and insertion of monomer into the tin alkoxide bond of the initiator (see Scheme 1).^{24–27} Kowalski et al. directly observed macromolecules containing tin alkoxide species in a polyester chain by MALDI-TOF mass spectroscopy. To ascertain whether this mechanism also applies in scR22 , we initiated the polymerization of L-LA with DoOH/ $\text{Sn}(\text{Oct})_2$ and in scR22 at 110 °C at 200 bar and followed the reaction by MALDI-TOF mass spectrometry. The MALDI-TOF mass spectrum of the L-LA/DoOH/ $\text{Sn}(\text{Oct})_2$ reacting mixture (Figure 1) shows that $\text{Do}-[\text{LA}]_n-\text{OH}$ chains are mainly formed. Figure 2 shows more detail of the spectrum, in which the fragments in Figure 1 for molar masses from 1040 to 1052 are shown (bold line) superimposed with the computed peaks for species having the composition $\text{C}_{12}\text{H}_{25}[\text{OCH}(\text{CH}_3)\text{CO}]_n\text{OSnO}(\text{O})\text{CC}_7\text{H}_{15}$, Na^+ . The agreement between the two shows that macromolecules containing tin alkoxide species ($\text{Do}-[\text{LA}]_n-\text{OSnOct}$) are present and, thus, that the polymerization of L-LA initiated by $\text{Sn}(\text{Oct})_2$ in scR22 proceeds via a coordination–insertion mechanism involving a covalent tin alkoxide active

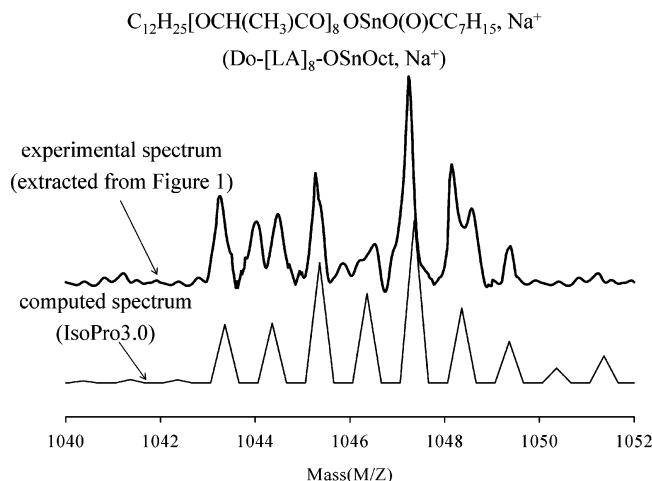


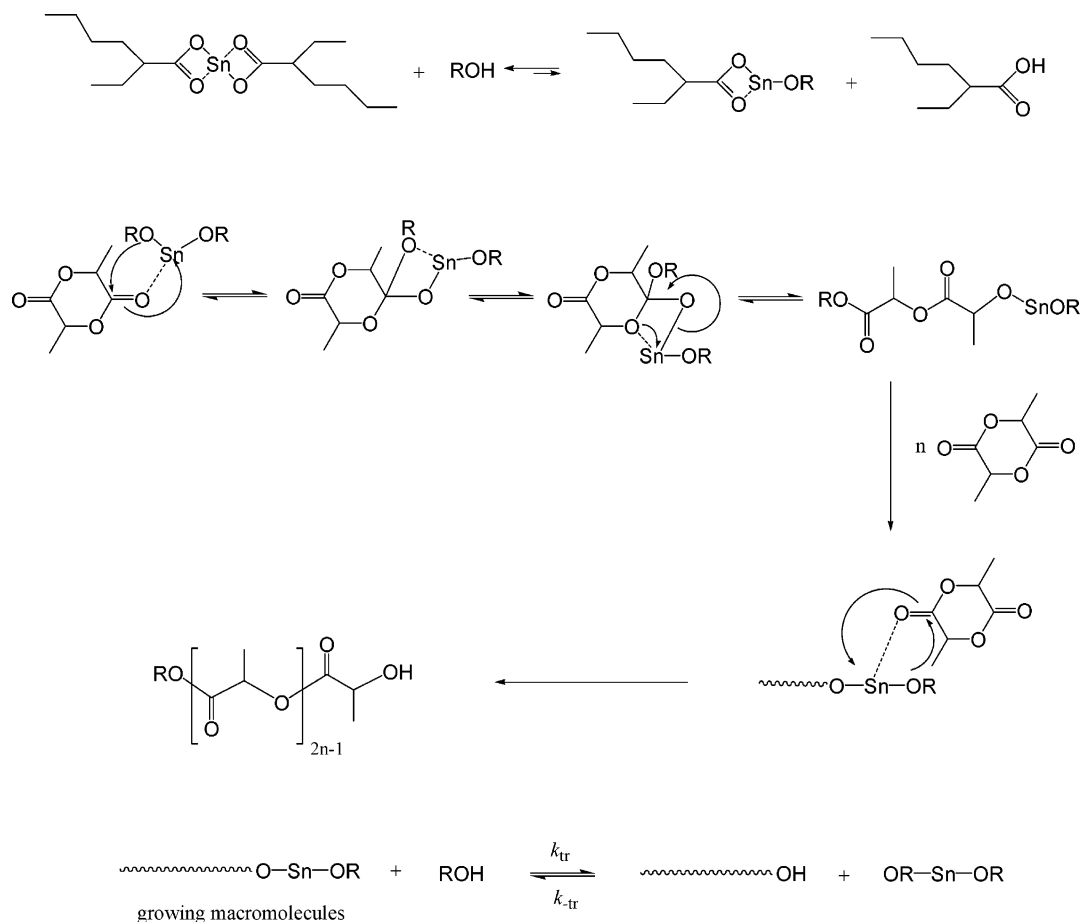
Figure 2. Comparison of the 1040–1052 m/z fragment of the MALDI-TOF spectrum shown in Figure 1 (bold line) with the isotopic distribution computed for the Do-[LA]₈-OSnOct, Na⁺ using the IsoPro3.0 program.

chain end. This observation is also consistent with the results of the following ¹H NMR spectroscopy study. The proton signals of the reaction mixture, obtained from above polymerization, are shown in Figure 3. The resonances of the methylene protons (peak *g*), adjacent to the hydroxyl group in DoOH, are shifted from 3.6 to 4.1 ppm (peak *g'*). The disappearance of peak *g* was monitored by measuring the intensity of the peak at 3.6 ppm. Peak *a''* belongs to the methine proton of L-LA at

the end of the polymer chain, observed as a quartet at 4.32 ppm. For a coordination–insertion mechanism, the ratio of the intensities of *g'* and *a''* ($I_{g'}/I_{a''}$) should be 2.0. The experimentally determined $I_{g'}/I_{a''}$ ratio (2.04) was in good agreement with this value.

Kinetics of L-LA Polymerization Initiated by DoOH/Sn(Oct)₂ in ScR22. The kinetics of L-LA polymerization initiated by Sn(Oct)₂ in the absence or in the presence of DoOH was studied in scR22 under a pressure of 200 bar. Figure 4 shows that while the monomer concentration decreased, as indicated by the peaks at 1.68 (*b*) and 5.02 ppm (*a*), the polymer signals increased, as seen from the peaks at 1.57 (*b'*) and 5.15 ppm (*a'*). From Table 1 and Figure 5, the kinetic data and plots obtained for the Sn(Oct)₂-initiated polymerization, produced a linear relationship in semilogarithmic coordinates within experimental error, where [LA]₀ and [LA] are the monomer concentrations at time zero (*t*₀) and *t*, respectively. Thus, the number of growing chains does not change appreciably during polymerization under the applied conditions. Furthermore, Figures 5 and 6 indicate that the polymerization process is a living process within the accuracy of our measurements, although the M_w/M_n ratio is much higher than expected from the Poisson distribution (cf. Table 1), which is probably due to increasing M_w due to bimolecular transesterification in the presence of a constant number of growing chains.²⁴ As the Sn(Oct)₂ concentration was increased, the relative polymerization rate constant (defined as $k_p = -d[LA]/[LA]dt = \ln([LA]_0/[LA])/t$, where *t* denotes the polymerization time) also increased from

Scheme 1. Coordination–Insertion Mechanism of L-Lactide Polymerization Initiated by ROH/Sn(Oct)₂, Including the Formation of the Tin Alkoxide Initiator, Showing Coordination–Insertion of the Monomer into the Tin Alkoxide Bond and Chain Transfer of the Active Macromolecules to Unreacted Alcohol



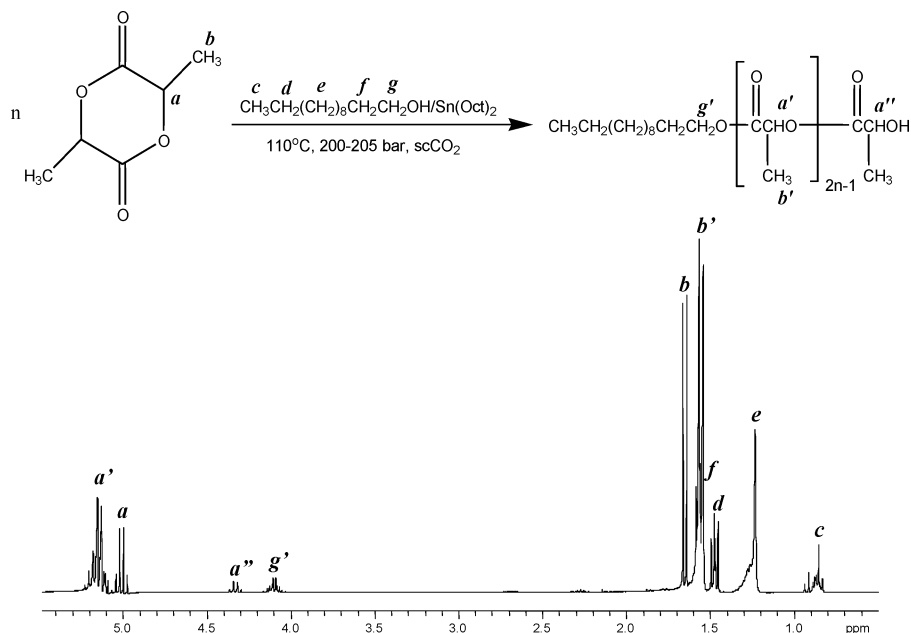


Figure 3. ^1H NMR spectrum of the crude reaction product obtained from L-lactide polymerization initiated by DoOH/Sn(Oct) $_2$. Polymerization conditions were as described in the caption of Figure 1.

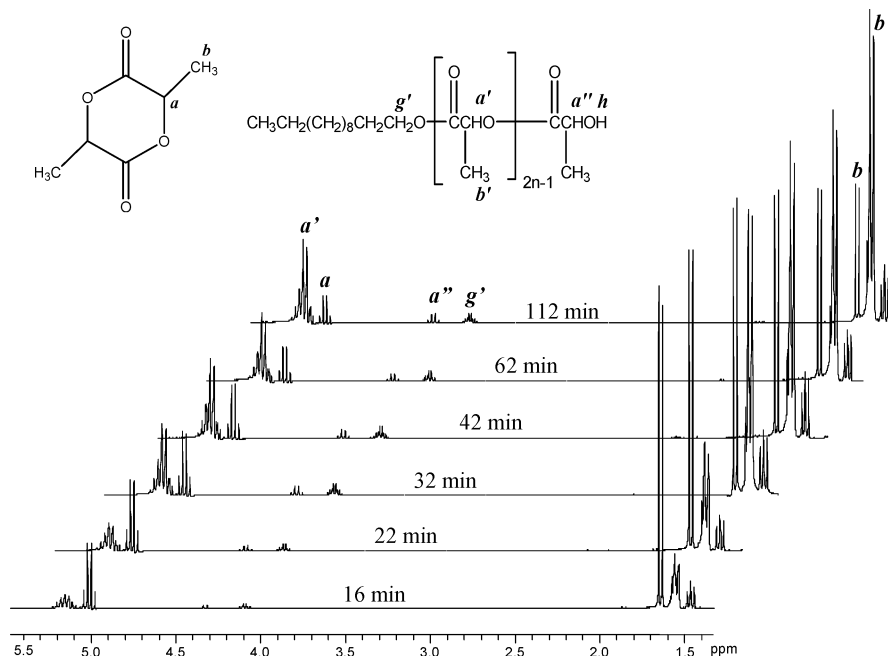


Figure 4. ^1H NMR spectra during the polymerization of L-lactide initiated by DoOH/Sn(Oct) $_2$. Polymerization conditions: $[\text{LA}]_0 = 0.4$ mol/L, $[\text{LA}]_0/[\text{DoOH}]_0 = 9.7$, and $[\text{DoOH}]_0/[\text{Sn}]_0 = 5.4$; in supercritical chlorodifluoromethane at 110 °C and 200 bar for various times.

$2.5 \times 10^{-3} \text{ min}^{-1}$ at $[\text{LA}]_0/[\text{Sn}]_0 = 406$ up to $22.0 \times 10^{-3} \text{ min}^{-1}$ at $[\text{LA}]_0/[\text{Sn}]_0 = 100$. These results mean that an adventitious co-initiator, i.e., a compound containing a hydroxyl group which is able to form a tin alkoxide active species, does exist in Sn(Oct) $_2$ itself. Increases in the initial concentration of Sn(Oct) $_2$ essentially increased the overall number of active chain ends and resulted in higher polymerization rates and shorter reaction times. These results are consistent with a polymerization mechanism with a rate that is dependent on the concentration of tin alkoxide.²⁶ For $[\text{LA}]_0/[\text{Sn}]_0 = 406$, $M_{n,\text{GPC}}$ of the resulting PLLA product was found to be 172 600 g/mol.¹¹

Polymerization was carried out in the presence of DoOH as co-initiator (see Table 2). In each case, the Sn-

(Oct) $_2$ concentration remained constant ($[\text{Sn}]_0 = 5.2 \times 10^{-5} \text{ mol/L}$, $[\text{LA}]_0/[\text{Sn}]_0 = 406$), and the DoOH concentration was varied. The polymerization rates increased from $2.5 \times 10^{-3} \text{ min}^{-1}$ at $[\text{DoOH}]_0/[\text{Sn}]_0 = 0$ up to $3.6 \times 10^{-3} \text{ min}^{-1}$ at $[\text{DoOH}]_0/[\text{Sn}]_0 = 1.9$, giving a k_p of 3.6×10^{-3} and $3.5 \times 10^{-3} \text{ min}^{-1}$ at $[\text{DoOH}]_0/[\text{Sn}]_0 = 3.1$ and 10.6, respectively (see Figure 7). These results indicate that the polymerization rate increased when DoOH was added. In detail, the polymerization rates increased with increasing DoOH initial concentration up to $[\text{DoOH}]_0/[\text{Sn}]_0 < 2$, and then the polymerization rate became independent of the initial DoOH concentration with $[\text{DoOH}]_0/[\text{Sn}]_0 > 2$. Recently, Penczek et al.^{24,27} observed similar rate behavior in Sn(Oct) $_2$ /alcohol-initiated polymerizations of ϵ -caprolactone in THF conducted at 80

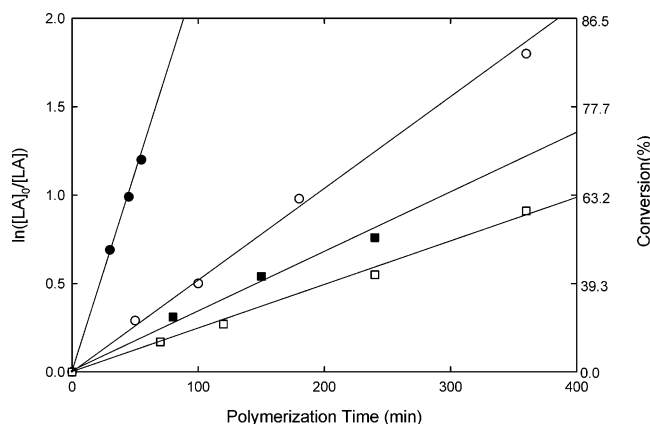


Figure 5. Kinetics of L-lactide polymerization in supercritical chlorodifluoromethane initiated by tin(II) octoate at 110 °C under 200 bar. $[LA]_0/[Sn]_0$ was (●) 100 ($k_p = 22.0 \times 10^{-3} \text{ min}^{-1}$), (○) 197 ($k_p = 5.2 \times 10^{-3} \text{ min}^{-1}$), (■) 295 ($k_p = 3.4 \times 10^{-3} \text{ min}^{-1}$), and (□) 406 ($k_p = 2.5 \times 10^{-3} \text{ min}^{-1}$). The other conditions were as described in the footnote of Table 1.

Table 1. Ring-Opening Polymerization of L-LA in Supercritical Chlorodifluoromethane at 110 °C and 200 bar Initiated by $\text{Sn}(\text{Oct})_2$ ^a

entry	$[LA]_0/[Sn]_0$	react time (min)	conv (%)	$M_{n,\text{GPC}}/10^3$ (g/mol)	MWD
1	406	70	15.6	29.6	1.21
2	406	120	23.7	45.0	1.23
3	406	240	42.3	74.9	1.26
4	406	360	59.7	126.2	1.33
5	406	480	62.5	138.0	1.38
6	406	600	67.0	146.0	1.38
7	406	1000	71.2	172.6	1.49
8	406	1200	71.5	171.5	1.50
9	295	80	26.5	38.7	1.16
10	295	150	42.1	70.2	1.22
11	295	240	53.0	91.2	1.34
12	197	50	25.2	36.2	1.29
13	197	100	39.4	49.5	1.35
14	197	180	62.5	76.3	1.36
15	100	30	50.0	48.1	1.17
16	100	46	62.8	60.5	1.28
17	100	55	69.9	68.7	1.29

^a CR_{22} (R22 concentration) is 40.8% w/v, $[LA]_0$ initial L-LA concentration is 0.4 mol/L, and $[Sn]_0$ initial $\text{Sn}(\text{Oct})_2$ concentration.

°C. They attributed their result to a propagation mechanism involving not the monomer– $\text{Sn}(\text{Oct})_2$ complex,²⁸ i.e., an “activated monomer mechanism”, but rather one due to monomer insertion at the active, tin alkoxide chain ends. A continuous increase in the rate would be expected to take place on increasing the initial alcohol concentration, provided that an “activated monomer” polymerization mechanism is applied. More recently, Storey et al.²⁶ reported that 2 mol of alcohol is required to fully react with $\text{Sn}(\text{Oct})_2$ to produce the active tin alkoxide initiator (see Scheme 1). After all the $\text{Sn}(\text{Oct})_2$ has been converted to tin alkoxide, no additional active polymerizing centers are present, provided the $[Sn]_0$ level remains constant. Thus, we concluded that the kinetics of L-LA polymerization in scR22 are in agreement with the above published works.

Comparison of ROP of L-LA in ScR22 with in Bulk. We also investigated the kinetics of the ROP of L-LA reaction in bulk (Table 3). In Figure 8, the first-order kinetic plots for ROP in scR22 and in bulk were compared. The straight lines characteristic of the bulk polymerization were found to have a much steeper slope than those of scR22. The difference in the polymeriza-

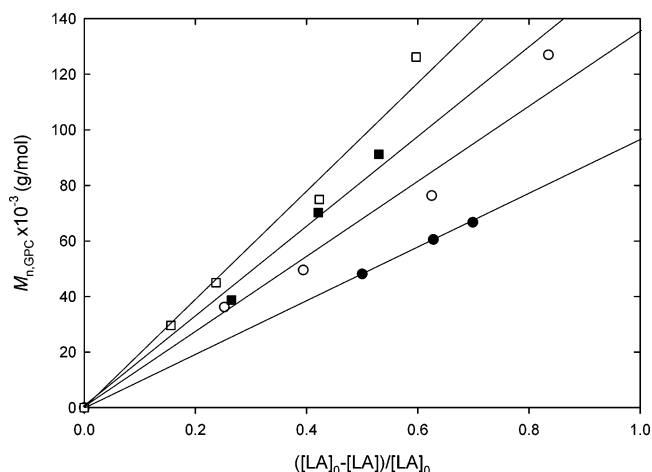


Figure 6. Dependence of the molecular weight (M_n) of poly(L-lactide) as determined by GPC on the degree of monomer conversion. Polymerization conditions: $[LA]_0 = 0.4 \text{ mol/L}$, 110 °C, 200 bar in supercritical chlorodifluoromethane; $[LA]_0/[Sn]_0$ was (●) 100, (○) 197, (■) 295, and (□) 406.

Table 2. Ring-Opening Polymerization of L-LA in Supercritical Chlorodifluoromethane at 110 °C and 200 bar Initiated by $\text{DoOH}/\text{Sn}(\text{Oct})_2$ ^a

entry	$[\text{DoOH}]_0/[Sn]_0$	react time (min)	conv (%)	$M_{n,\text{GPC}}/10^3$ (g/mol)	MWD
18	0	100	22.1	44.1	1.23
19	0	220	41.5	74.0	1.28
20	0	350	59.0	116.2	1.35
21	0.3	180	40.1	32.5	1.28
22	0.3	250	49.3	41.1	1.38
23	0.3	300	56.9	61.2	1.49
24	1.3	180	46.9	37.0	1.49
25	1.3	250	54.1	44.0	1.51
26	1.3	320	62.8	67.2	1.55
27	1.9	200	52.2	39.1	1.56
28	1.9	300	65.1	65.3	1.62
29	1.9	420	76.9	81.2	1.72
30	3.1	220	51.0	31.5	1.70
31	3.1	300	66.0	59.0	1.75
32	3.1	420	75.2	73.3	1.82

^a CR_{22} (R22 concentration) 40.8% w/v, $[LA]_0$ initial L-LA concentration 0.4 mol/L, $[\text{DoOH}]_0$ initial DoOH concentration, $[Sn]_0$ initial $\text{Sn}(\text{Oct})_2$ concentration, and $[LA]_0/[Sn]_0 = 406$.

tion rate constants was large. Indeed, applying $[\text{DoOH}]_0/[Sn]_0 = 0$, k_p is $12.0 \times 10^{-3} \text{ min}^{-1}$ in bulk and $2.5 \times 10^{-3} \text{ min}^{-1}$ in scR22. Therefore, on the basis of the k_p values, the polymerization at 110 °C is ca. 5 times faster in bulk than in scR22. It is known that propagating active species tends to associate in bulk and in solutions of apolar solvents and that the mean degree of association is controlled by the polarity and the coordinating capability of the solvent.²⁹ Teyssié et al.²⁰ reported that when lactide is polymerized in THF, there is competition between the monomer and solvent for coordination to active species, which explains why polymerization is slower in THF than in toluene. Recently, Jérôme et al.^{22,23} also observed a similar behavior, i.e., a decrease of k_p in scCO_2 , in the dibutyltin dimethoxide-initiated polymerization of ϵ -caprolactone conducted at 40 °C and 210 bar. They attributed their result to the formation of dormant species, i.e., carbonated tin alkoxide species, and this was confirmed by infrared analysis. The carbonation reaction, which results in a positive volume of activation and a higher energy of activation versus polymerization in a regular hydrocarbon solvent, slows down the polymerization rate. Therefore, in the present study chlorodifluoromethane and the ester carbonyl

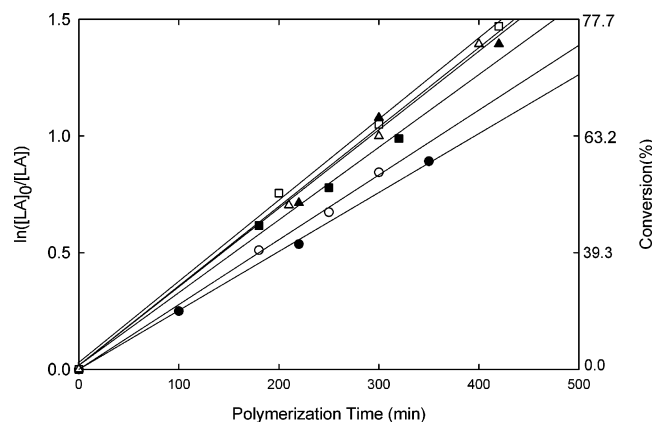


Figure 7. Kinetics of L-lactide polymerization in supercritical chlorodifluoromethane initiated by 1-dodecanol/tin(II) octoate. The $[LA]_0/[Sn]_0$ was constant as 406 and $[DoOH]_0/[Sn]_0$ was (●) 0 ($k_p = 2.5 \times 10^{-3} \text{ min}^{-1}$), (○) 0.3 ($k_p = 2.8 \times 10^{-3} \text{ min}^{-1}$), (■) 1.3 ($k_p = 3.2 \times 10^{-3} \text{ min}^{-1}$), (○) 1.9 ($k_p = 3.6 \times 10^{-3} \text{ min}^{-1}$), (▲) 3.1 ($k_p = 3.6 \times 10^{-3} \text{ min}^{-1}$), and (△) 10.6 ($k_p = 3.5 \times 10^{-3} \text{ min}^{-1}$). Other conditions were as described in the footnote of Table 2.

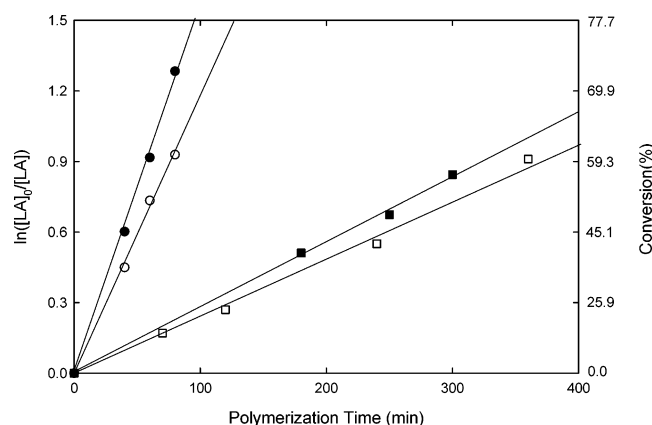


Figure 8. Kinetics of L-lactide polymerization in supercritical chlorodifluoromethane initiated by 1-dodecanol/tin(II) octoate. Conditions of polymerization: $[LA]_0 = 0.42 \text{ mol/L}$ ($[LA]_0/[Sn]_0 = 406$), 110°C in bulk (● and ○) and $[LA]_0 = 0.4 \text{ mol/L}$, 110°C , 200 bar in scR22 (■ and □); $[DoOH]_0/[Sn]_0$ was (●) 0.6 ($k_p = 16.0 \times 10^{-3} \text{ min}^{-1}$), (○) 0 ($k_p = 12.0 \times 10^{-3} \text{ min}^{-1}$), (■) 0.3 ($k_p = 2.8 \times 10^{-3} \text{ min}^{-1}$), and (□) 0 ($k_p = 2.5 \times 10^{-3} \text{ min}^{-1}$).

Table 3. Ring-Opening Polymerization of L-LA in Bulk at 110°C Initiated by $DoOH/Sn(Oct)_2$ ^a

entry	$[LA]_0/[Sn]_0$	$[DoOH]_0/[Sn]_0$	react time (min)	conv (%)	$M_{n,GPC}/10^3$ (g/mol)	MWD
33	100	0	15	50.3	57.1	1.19
34	100	0	25	69.2	98.1	1.20
35	100	0	35	78.5	106.8	1.27
36	197	0	25	39.4	80.2	1.20
37	197	0	50	64.6	122.9	1.25
38	197	0	59	70.0	142.2	1.31
39	406	0	40	36.2	95.0	1.17
40	406	0	60	52.0	120.5	1.26
41	406	0	80	60.5	136.2	1.28
42	406	0.6	40	45.2	39.8	1.18
43	406	0.6	60	60.0	56.3	1.23
44	406	0.6	80	72.3	64.7	1.24

^a $[LA]_0$ initial L-LA concentration is 0.4 mol/L, $[DoOH]_0$ initial DoOH concentration, and $[Sn]_0$ initial $Sn(Oct)_2$ concentration.

group of the monomer may have competed for coordination onto the tin of the initiator, which would explain the slower kinetics than in bulk.

For $[DoOH]_0/[Sn]_0 = 0.3$ in scR22, $M_{n,GPC}$ of the resulting PLLA product was determined to be 126 000

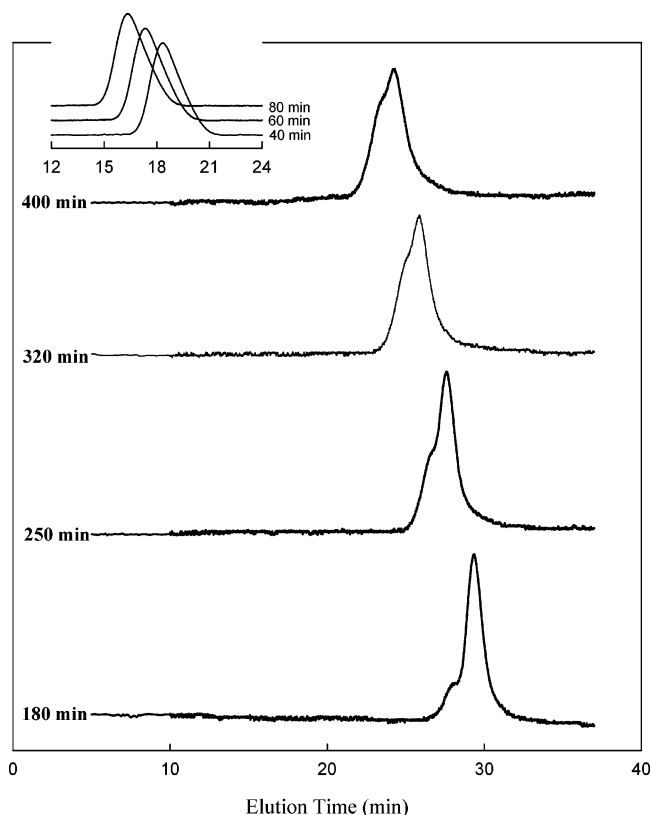


Figure 9. GPC curves of PLLA initiated by $DoOH/Sn(Oct)_2$ ($[LA]_0/[Sn]_0 = 406$ and $[DoOH]_0/[Sn]_0 = 1.3$) after 180, 250, 320, and 400 min in scR22. Monomer conversions were 46.9, 54.1, 62.8, and 67.0%, respectively. MWD values were 1.49, 1.51, 1.55, and 1.62, respectively; inset shows GPC curves without a bimodal PLLA MWD produced by bulk polymerization initiated by $DoOH/Sn(Oct)_2$ ($[LA]_0/[Sn]_0 = 406$ and $[DoOH]_0/[Sn]_0 = 1.3$) for various reaction times.

g/mol (DP = 880); i.e., the calculated concentration of macromolecules ($[LA]_0/DP$) was equal to $4.5 \times 10^{-4} \text{ mol/L}$, which is slightly higher than the concentration of the alcohol added ($[DoOH]_0 = 3.1 \times 10^{-4} \text{ mol/L}$). On the other hand, for bulk polymerization at the same molar ratio, $M_{n,GPC}$ of the resulting PLLA product was determined to be 191 000 g/mol; i.e., the calculated concentration of the macromolecules was equal to $3.0 \times 10^{-4} \text{ mol/L}$, which is actually the same as the concentration of the alcohol added ($[DoOH]_0 = 3.1 \times 10^{-4} \text{ mol/L}$). This result indicates that an adventitious co-initiator; i.e., moisture in the R22 itself has reduced the M_n of the resulting PLLA.

The linear nature of the data in Figure 7 suggests that the polymerization of L-LA in scR22 by $DoOH/Sn(Oct)_2$ is controlled. However, GPC analysis indicated that, interestingly enough, the resulting molecular weight distribution (MWD) is not monomodal but bimodal, at least at certain conversions. As the monomer conversions increased, these peaks tended to merge into a single broad peak (see Figure 9). Specifically, the relative intensities of broad peaks with low elution volumes continuously increased, and narrow peaks with high elution volumes continuously shifted toward low elution volume and merged into a broad peak at low elution volume. On the other hand, monomodal MWD was obtained by bulk polymerization (see inset in Figure 9). Broadening of the MWD may be due to slow initiation, chain transfer to monomer, intra-/intermolecular chain transfer,²¹ and multiplicity of the active sites (exchanging slowly).^{30,31} If intra-/intermolecular trans-

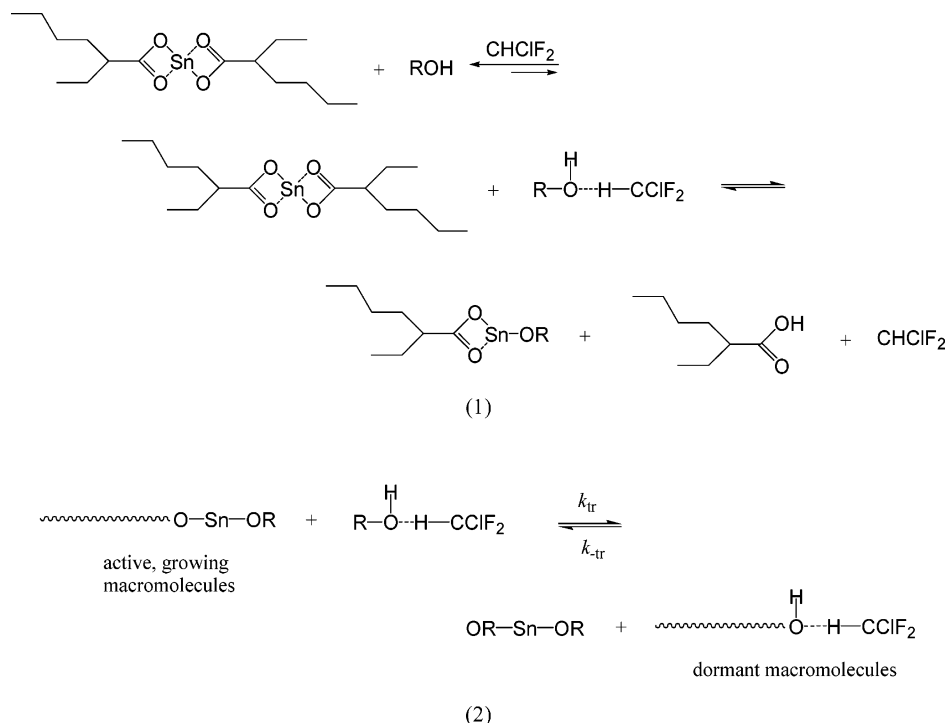


Figure 10. Mechanism illustrating (1) the cross-association between the hydrogen on R22 and the hydroxyl end groups on ROH (DoOH), hindering $\text{Sn}(\text{Oct})_2$ and ROH from converting into tin alkoxide, and (2) the cross-association between the hydrogen on R22 and the hydroxyl end groups on macromolecules to form temporarily dormant macromolecules. The macromolecules with hydroxyl end groups are produced by a chain transfer reaction between active macromolecules and unreacted alcohol.

esterification effectively competes with the ring-opening polymerization of lactone, the MWD of the isolated polymers should broaden with increasing conversion and MWD should be bimodal.³² In the present study, however, a bimodal MWD was also observed during the initial stages at low conversion. Matyjaszewski et al.³⁰ reported that a chain polymerization with a variety of active species propagating simultaneously yields polymers with a broad or polymodal molecular weight distribution. The bimodality can be explained by the fact that during these conversions two coexisting populations of polymer chains are present. Thus, we concluded that when $\text{Sn}(\text{Oct})_2$ reacts with DoOH and is converted into tin alkoxide, this may be an equilibrium reaction and have differences in lifetimes with intermolecular interactions between ROH (DoOH) and R22 (see (1) in Figure 10), such that the tin alkoxide concentration in R22 is temporarily lower than system without R22, i.e., bulk polymerization. Similarly, in terms of intermolecular chain transfer, active macromolecules may be in equilibrium with temporarily dormant species by reversibly displacing active macromolecules from Sn atoms, and both active and dormant species may have different lifetimes (see (2) in Figure 10). Because of the hindered tin alkoxide formation and chain transfer to temporarily dormant macromolecules, the bimodal MWD was observed when scR22 was used as reaction medium. When the growing, active macromolecules become temporarily dormant and exchange slowly, the number of polymer chains remains constant but their distribution changes. In addition, the shape and breadth of MWD are dependent on the relative rates of exchange between dormant and active species and on the lifetimes of both species.

This conclusion is supported by the following observation. Gregg et al.³³ described the phase behavior of favorable interactions between the hydroxyl group and

R22. From studies of cloud point measurements in R22 from -50 to 200 °C up to 400 bar, these authors found that as hydroxyl groups were added to alkyl chains/polymers (e.g., $\text{CH}_3\text{-R}'\text{-CH}_3$, $\text{HO-R}'\text{-CH}_3$, and $\text{HO-R}'\text{-OH}$), the phase-boundary pressures for the above materials essentially coincided over the entire temperature range investigated due to the cross-association between the hydroxyl groups on alkyl chains/polymers and the hydrogen on R22. In contrast, in nonpolar CO_2 solution, the phase-boundary pressures shifted on adding hydroxyl groups to the polymer due to the formation of hydrogen-bonded polymer aggregates formed by self-association.³³ Therefore, the cross-association between the hydrogen on chlorodifluoromethane and the hydroxyl end group on DoOH and on macromolecules ($\text{R-OH} \cdots \text{H-CClF}_2$) may temporarily reduce the tin alkoxide and the growing macromolecule concentrations.

Conclusions

When the ring-opening polymerization of L-LA initiated by DoOH/ $\text{Sn}(\text{Oct})_2$ was carried out in scR22, polymerization proceeded via a traditional coordination-insertion mechanism involving tin alkoxide bond formation and cleavage of the acyl-oxygen bond of the monomer. In detail, $\text{Sn}(\text{Oct})_2$ reacts with DoOH and is converted into tin alkoxide. This may be an equilibrium reaction and had differences in lifetimes with the intermolecular interaction between ROH and scR22, such that the tin alkoxide concentration may be temporarily lower than that of the bulk polymerization. Similarly, in terms of intermolecular chain transfer, active macromolecules may be in equilibrium with temporarily dormant species. A bimodal MWD was observed when scR22 was used as a reaction medium, which may be due to the above-mentioned hindered tin alkoxide formation and chain transfer to temporarily

dormant macromolecules with slow exchange. When the growing, active macromolecules convert into a temporarily dormant form, exchanging slowly, the number of chains remains constant but their distribution changes.

Acknowledgment. The authors are grateful to the Ministry of Commerce, Industry and Energy, Korea, for its support (Project No. 10011159).

Supporting Information Available: Text and figures giving the details of the phase behavior of PLLA in R22 as a function of molecular weights. This material is available free of charge via the Internet at <http://pubs.acs.org>.

References and Notes

- (1) (a) Eckert, C. A.; Knutson, B. L.; Debenedetti, P. G. *Nature (London)* **1996**, *373*, 313. (b) Leitner, W. *Nature (London)* **2000**, *405*, 129.
- (2) (a) Canelas, D. A.; DeSimone, J. M. *Adv. Polym. Sci.* **1997**, *133*, 103. (b) Kendall, J. L.; Canelas, D. A.; Young, J. L.; DeSimone, J. M. *Chem. Rev.* **1999**, *99*, 543.
- (3) Cooper, A. I. *J. Mater. Chem.* **2000**, *10*, 207.
- (4) Sarbu, T.; Styranec, T.; Beckman, E. J. *Nature (London)* **2000**, *405*, 165.
- (5) (a) DeSimone, J. M.; Guan, Z.; Elsbernd, C. S. *Science* **1992**, *257*, 945. (b) Shah, V. M.; Hardy, B. J.; Stern, S. A. *J. Polym. Sci., Part B: Polym. Phys.* **1993**, *31*, 313. (c) Ehrlich, P. *Chemtracts: Org. Chem.* **1993**, *6*, 92. (d) Kapellen, K. K.; Mistele, C. D.; DeSimone, J. M. *Macromolecules* **1996**, *29*, 495. (e) van Herk, A. M.; Manders, B. G.; Canelas, D. A.; Quadir, M.; DeSimone, J. M. *Macromolecules* **1997**, *30*, 4780.
- (6) (a) DeSimone, J. M.; Maury, E. E.; Menciloglu, Y. Z.; McClain, J. B.; Romack, T. J.; Combes, J. R. *Science* **1994**, *265*, 356. (b) Christian, P.; Giles, M. R.; Griffiths, R. M. T.; Irvine, D. J.; Major, R. C.; Howdle, S. M. *Macromolecules* **2000**, *33*, 9222. (c) Shiho, H.; DeSimone, J. M. *Macromolecules* **2001**, *34*, 1198. (d) Li, G.; Yates, M. Z.; Johnston, K. P.; Howdle, S. M. *Macromolecules* **2000**, *33*, 4008. (e) Giles, M. R.; Griffiths, R. M. T.; Aguiar-Ricardo, A.; Silva, M. M. C. G.; Howdle, S. M. *Macromolecules* **2001**, *34*, 20. (f) Wood, C. D.; Cooper, A. I.; *Macromolecules* **2001**, *34*, 5. (g) Fehrenbacher, U.; Ballauff, M. *Macromolecules* **2002**, *35*, 3653.
- (7) Lee, J. M.; Lee, B.-C.; Lee, S.-H. *J. Chem. Eng. Data* **2000**, *45*, 851.
- (8) Lee, J. M.; Lee, B.-C.; Hwang, S.-J. *J. Chem. Eng. Data* **2000**, *45*, 1162.
- (9) Kuk, Y.-M.; Lee, B.-C.; Lee, Y.-W.; Lim, J. S. *J. Chem. Eng. Data* **2002**, *44*, 575.
- (10) Conway, S. E.; Byun, H.-S.; Mchugh, M. A.; Wang, J. D.; Mandel, F. S. *J. Appl. Polym. Sci.* **2001**, *80*, 1155.
- (11) Pack, J. W.; Kim, S. H.; Park, S. Y.; Lee, Y.-W.; Kim, Y. H. *Macromolecules*, **2003**, *36*, 7884.
- (12) Because of their oxidation in the troposphere, R22 has a lower half-life than chlorofluoromethanes (CFCs) and therefore a lower ozone depletion potential. See: (a) Ravishankara, A. R.; Turnipseed, A. A.; Jensen, N. R.; Barone, S.; Mills, M.; Howard, C. J.; Solomon, S. *Science* **1994**, *263*, 71. (b) First Review Meeting of Parties to the 1987 Montreal Protocol on Substances that Deplete the Ozone Layer, London, June 1990, and Copenhagen, 1992. (c) Powell, R. L. *J. Fluorine Chem.* **2002**, *114*, 237 and references therein.
- (13) Wood, C. D.; Senoo, K.; Martin, C.; Cuellar, J.; Cooper, A. I. *Macromolecules* **2002**, *35*, 6743.
- (14) Dubois, Ph.; Jacobs, Ch.; Jérôme, R.; Teyssié, Ph. *Macromolecules* **1991**, *24*, 2266.
- (15) Leenslag, J. W.; Pennings, A. J. *Makromol. Chem.* **1987**, *188*, 1809.
- (16) Kricheldorf, H. R.; Kreiser-Saunders, I.; Stricker, A. *Macromolecules* **2000**, *33*, 702.
- (17) Zhang, X.; MacDonald, D. A.; Goosen, M. F. A.; McAuley, K. B. *J. Polym. Sci., Part A: Polym. Chem.* **1994**, *32*, 2965.
- (18) Storey, R. F.; Taylor, A. E. *J. Macromol. Sci., Pure Appl. Chem.* **1996**, *A33*, 77; **1998**, *A35*, 723.
- (19) Ryner, M.; Stridsberg, K.; Albertsson, A.-C.; von Schenck, H.; Svensson, M. *Macromolecules* **2001**, *34*, 3877.
- (20) Ropson, N.; Dubois, Ph.; Jérôme, R.; Teyssié, Ph. *Macromolecules* **1995**, *28*, 7589.
- (21) Kricheldorf, H. R.; Berl, M.; Scharnagl, N. *Macromolecules* **1988**, *21*, 286.
- (22) Stassin, F.; Halleux, O.; Jérôme, R. *Macromolecules* **2001**, *34*, 775.
- (23) Stassin, F.; Jérôme, R. *Chem. Commun.* **2003**, *2*, 232.
- (24) Kowalski, A.; Duda, A.; Penczek, S. *Macromol. Rapid Commun.* **1998**, *19*, 567.
- (25) Kowalski, A.; Duda, A.; Penczek, S. *Macromolecules* **2000**, *33*, 689.
- (26) Storey, R. F.; Sherman, J. W. *Macromolecules* **2002**, *35*, 1504.
- (27) Kowalski, A.; Duda, A.; Penczek, S. *Macromolecules* **2000**, *33*, 7359.
- (28) (a) Du, Y. J.; Lemstra, P. J.; Nijenhuis, A. J.; van Aert, H. A. M.; Bastiaansen, C. *Macromolecules* **1995**, *28*, 2124. (b) Kricheldorf, H. R.; Kreiser-Saunders, I.; Boettcher, C. *Polymer* **1995**, *36*, 1253.
- (29) (a) Ouhadi, T.; Stevens, C.; Teyssié, Ph. *Makromol. Chem., Suppl.* **1975**, *1*, 191. (b) Shiner, V. J.; Whittaker, D.; Fernandez, V. P. *J. Am. Chem. Soc.* **1963**, *85*, 2318. (c) Akitt, J. W.; Dunlan, R. H. *J. Magn. Reson.* **1975**, *15*, 162.
- (30) Matyjaszewski, K.; Szymanski, R.; Teodorescu, M. *Macromolecules* **1994**, *27*, 7565.
- (31) Baran, J.; Duda, A.; Kowalski, A.; Szymanski, R.; Penczek, S. *Macromol. Rapid Commun.* **1997**, *18*, 325.
- (32) Chamberlain, B. M.; Jazdzewski, B. A.; Pink, M.; Hillmyer, M. A.; Tolman, W. B. *Macromolecules* **2000**, *33*, 3970.
- (33) Gregg, C. J.; Stein, F. P.; Radosz, M. *J. Phys. Chem. B* **1999**, *103*, 1167.

MA034910N